doi: 10.15407/ujpe62.05.0413

YU.P. MAZUR, R.V. OSTAPENKO, M.P. SEMEN'KO

Taras Shevchenko National University of Kyiv, Faculty of Physics
(64/13, Volodymyrs'ka Str., Kyiv 01601, Ukraine; e-mail: smp@univ.kiev.ua)

PACS 72.15.Eb, 61.43.-j, 61.72.Cc, 61.46.-w, 61.72.Hh

INFLUENCE OF A COLD PLASTIC DEFORMATION ON THE ELECTRICAL RESISTIVITY OF CrMnFeCoNi HIGH-ENTROPY ALLOY

The influence of a cold rolling deformation on the electrical transport properties of CrMnFeCoNi high-entropy alloy (HEA) has been studied. It is shown that the growth of the strain ε at rolling gives rise to a decrease of the alloy electrical resistivity ρ and an increase of the temperature coefficient of resistance α. The X-ray diffraction study did not reveal any phase changes at that. Such dependences of ρ and α on ε differ from the behavior of those parameters in the majority of ordinary metal alloys. The temperature dependence of the electrical resistance of deformed samples at their heating is found to have an abnormal S-like shape. Using the positions of such S-anomalies obtained at different heating rates, the activation energy E_a of the process responsible for the appearance of this anomaly is determined with the help of the Kissinger method. The form of the dependence $\rho(T)$ and the value of E_a give us ground to connect the specific features in the behavior of ρ in deformed specimens with the existence of a "K-state" in the examined HEA, which emerges in some deformed alloys based on transition metals. Possible thermodynamic reasons for the appearance of this state have been discussed.

K e y w o r d s: high-entropy alloy, electrical resistivity, K-state, plastic deformation, structure.

1. Introduction

As a rule, traditional metal alloys include one or two metal components. The parameters of a basic alloy are practically always modified by introducing doping additives. The amount of the latter can be considerable, but their content remains relatively low. An essentially new class of metal alloys has been obtained rather recently; they were called high-entropy alloys (HEAs) [1]. The composition of the alloys belonging to the new class consists of five or more metal components. However, unlike traditional metal alloys, their content is close to equiatomic [2].

Despite such a large number of components, the crystalline structure of HEAs is rather simple: this is either the bcc or fcc phase with parameters that are close to those of pure metals or traditional alloys on their basis [2]. The composition and the simple type of crystal structure allow HEAs to be classed to solid substitutional solutions, though the terms "solvent" and "dissolved atom" are evidently not clear in this case.

Owing to their specific physical, chemical, and mechanical properties, HEAs are very promising for engineering applications, first of all, as heat-resistant [3], wearproof [4], and constructional materials [5], as anticorrosive materials [6], and owing to their ability to play the role of diffusion barriers [7]. At the same time, they can also be applied in other spheres. In particular, the magnetic properties of those materials can change from ferromagnetic to paramagnetic and superparamagnetic, as their composition is varied [8, 9]. Some of the alloys concerned can be applied as magnetically soft alloys [2, 8].

In addition, HEAs possess specific electrical properties, which deserve attention. Unlike pure metals and the vast majority of traditional alloys, for which the resistivity ρ is low, the mobility of charge carriers is rather high, and the thermal coefficient of resistance (TCR) α is large, HEAs are characterized by large ρ-values (90–100 $\mu\Omega \cdot$ cm) [10–13], low Hall mobilities of charge carriers (0.4–2.61 $\mathrm{cm}^2/(\mathrm{V} \cdot \mathrm{s})$) [13], and relatively low α (about 10^{-4} K^{-1}), despite that they have practically the same concentrations of charge carriers as pure metals [13]. Even if the advantages of other physico-chemical and mechanical properties are not taken into consideration, a low TCR magnitude and a high resistivity of HEAs satisfy the requirements established for the materials that are used in precision electronic devices such as reference resistances, strain gauges, thermocouples, and others.

Although HEAs have been known for more than a decade, there are not many works dealing with the research of the electrical resistivity in those materials (in addition to works [10–13], only a few ones can be mentioned). The main features of the electric resistivity are assumed to be governed by the conventional phonon mechanism, in which the strong imperfection of the structure associated with a large number of HEA components is taken into account [5, 6]. However, this is only a superficial viewpoint, because the body of experimental data is insignificant. Therefore, on the basis of electric properties, the mechanism of electric resistivity in HEAs can be regarded, on the same footing, to be rather close to that in amorphous alloys and semimetals.

In order to refine the mechanisms of scattering in HEAs, this work contains the results of our research concerning the influence of a cold plastic deformation on the resistivity in one of the known representatives of HEAs: CrMnFeCoNi alloy.

2. Experimental Materials and Methods

CrMnFeCoNi high-entropy alloys prepared from chemically pure elements by melting blends with corresponding compositions in the electric arc in the pure argon environment are studied. The obtained ingot was remelted 6 to 7 times in order to homogenize its composition. Then the melt was poured out into a copper form 10 mm in diameter and 100 mm long, which was cooled with water. Experimental specimens with required dimensions were cut out from the obtained ingots.

The temperature dependences of the electrical resistance, $R(T)$, were studied with the use of specimens 20 mm long and with a transverse cross-section of 1×1 mm^2. The measurements were carried out, by following the standard four-probe technique in a temperature interval from 77 to 900 K. The structure and the phase composition were studied, by using the X-ray diffraction method on a DRON-4 diffractometer with the use of Co_{K_α}-radiation. For this purpose, specimens with dimensions not less than 7×7 mm^2 were used.

The plastic deformation of specimens was performed by means of the cold rolling. The squeezing strain ε was determined by the formula $\varepsilon = (d_0 - d)/d_0 \times 100\%$, where d_0 and d are the thicknesses of the initial and rolled specimens, respectively. The deformation effect was monitored qualitatively within the thermal emf method. In this case, the deformation-induced thermal emf was measured: it was determined by measuring the thermal emf at a fixed temperature difference of a thermocouple, with one of its branches being the reference material (Pb or the initial, i.e. unrolled, HEA), and the other was made of the deformed material.

3. Experimental Results

CrMnFeCoNi alloy is a typical representative of high-entropy alloys consisting of 3d-transition metals. The common features of the electric resistivity and some structural features of this alloy and $\mathrm{CrMnFeCoNi_2Cu}$ high-entropy alloy were studied in work [14]. CrMnFeCoNi high-entropy alloy is characterized by the fcc structure with the cell parameter $a = 0.3596(7)$ nm before a deformation. A specific feature in the initial alloy structure is the presence of a texture. Generally speaking, a texture is observed quite often in various HEAs, being evidently a consequence of technological processes. The resistivity of CrMnFeCoNi is rather high and amounts to $\rho_{300} = 109$ $\mu\Omega$ cm at $T = 300$ K, whereas the TCR is small and equals $\alpha_{300} = 4.0 \times 10^{-4}$ K^{-1} at $T = 300$ K.

In Fig. 1, a collection of X-ray diffraction patterns is shown, which were obtained for CrMnFeCoNi alloy deformed to various ε-values. One can see that the increase of ε results in the texture variation of examined specimens. In this case, the intensity of peak (111) increases, and that of peak (200) decreases. However, it

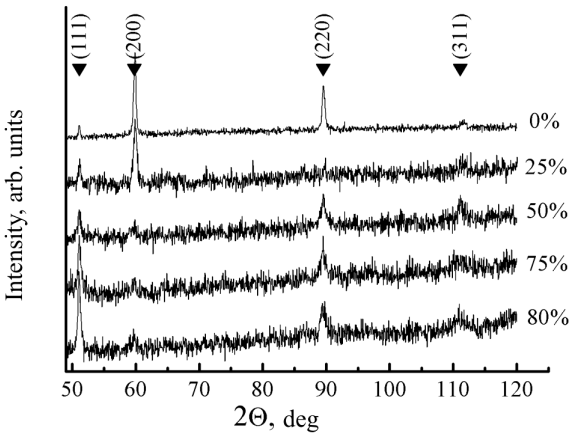

Fig. 1. Fragments of X-ray diffraction patterns obtained for CrMnFeCoNi high-entropy alloy after its deformation by rolling to various deformation strains ε (the corresponding ε-values are indicated near the diffraction patterns)

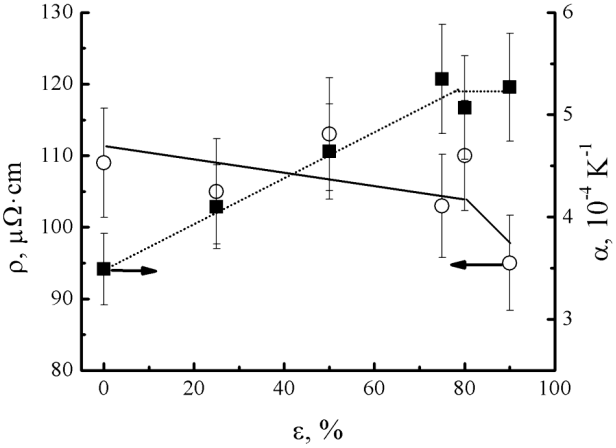

Fig. 2. Dependences of the specific electrical resistance ρ and the TCR α at $T = 300$ K on the deformation strain ε

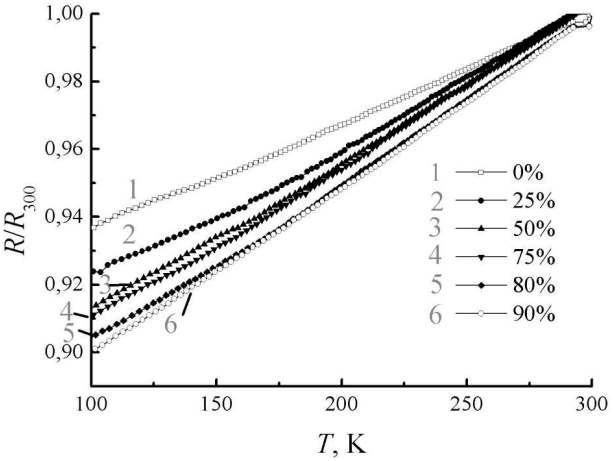

Fig. 3. Temperature dependences of the normalized resistance $R(T)/R_{300}$ in a temperature interval of 77–400 K for specimens rolled to various ε

is rather difficult to completely determine the structural parameters on the basis of those researches.

The calculation of the fcc lattice parameter a for various deformations showed that this quantity remains practically the same as before a deformation within the calculation error limits.

Figure 2 illustrates the evolution of the electric resistivity $\rho_{300} = \rho(T = 300$ K) with the growth of a strain ε. A level of 7% was taken for the measurement accuracy of the specific resistance, which reasonably corresponds to the measurement accuracy of ρ_{300} for rectangular specimens. Within the limits of this accuracy, one could have adopted that ρ_{300} does not depend on ε. However, in our opinion, this parameter most likely only slightly decreases in a strain interval of 0–80% and diminishes more strongly at larger deformations. Arguments for the existence of two such different sections in the dependence $\rho_{300}(\varepsilon)$ follow from the data obtained for the dependences of TCR and thermal emf on ε.

Fragments of the temperature dependences of the normalized resistance, $R(T)/R_{300}$, for specimens rolled to various ε-values are depicted in Fig. 3. For the informative purpose, a temperature interval of 77–400 K was shown. One can see rather well that the slope of the dependence $R(T)/R_{300}$ grows with ε, which testifies to the increase of TCR. The corresponding variations were determined quantitatively on the basis of the TCR magnitude at $T = 300$ K, α_{300}. The obtained $\alpha_{300}(\varepsilon)$ dependence, as well as the $\rho_{300}(\varepsilon)$ dependence, is plotted in Fig. 2 by black squares. A visible correlation between the dependences $\rho_{300}(\varepsilon)$ and $\alpha_{300}(\varepsilon)$ is quite reasonable and justifies the existence of two different sections in the strain dependences of those quantities mentioned above. A specific feature of both dependences is their unusual, opposite to the standard, behavior with the change of the strain value ε, because ρ, as a rule, has to grow, and the TCR, accordingly, to decrease at a deformation.

Figure 4 exhibits the ε-dependence of the thermal emf $\Delta S_T = S_T(\varepsilon) - S_T(0)$ that arises between the reference branch and the specimen deformed to various ε-values. As one can see, besides the thermal emf aris-

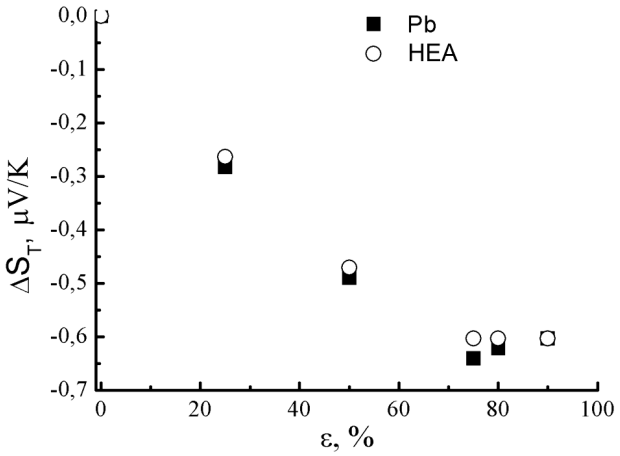

Fig. 4. Dependences of the additional deformation-induced thermal emf ΔS_T obtained with respect to the undeformed HEA (hollow circles) and lead (solid squares) on ε

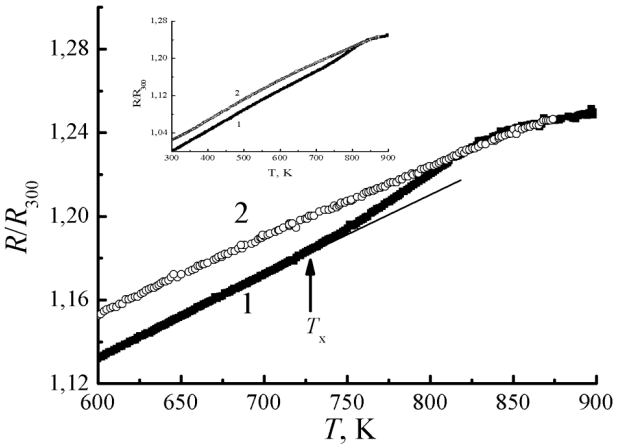

Fig. 5. Typical temperature dependences of the normalized electrical resistance R/R_{300} in the deformed HEA in a temperature interval of 600–900 K: the first heating cycle (*1*), the second heating cycle (*2*). The same dependences but in a temperature interval of 300–900 K are shown in the inset

ing between the pair of materials in the case with the reference Pb specimen, there emerges an additional emf, ΔS_T, which grows by magnitude for growing $\varepsilon < 80\%$. At strains $\varepsilon \geq 80\%$, the magnitude of ΔS_T practically does not change, i.e. it saturates. Those features in the behavior of the deformation-induced thermal emf are typical of metal systems and can be considered as a result of the accumulation of various defects in the deformed part of a thermocouple. Figure 4 also rather distinctly demonstrates the existence of two deformation sections.

The influence of a deformation on the charge transfer parameters and their temperature behavior, which was considered above, concerns either the room temperature or the temperatures below it. In a wider temperature interval (to 900 K), the $R(T)/R_{300}$ dependences for the initial (undeformed) CrMnFeCoNi high-entropy alloy contain no features. In the case of $CrMnFeCoNi_2Cu$ alloy, irreversible changes (reduction) in the electric resistivity due to the thermal action were revealed, which can be associated with the processes that run in this alloy owing to the presence of an additional fcc2 phase in it [14].

However, irreversible changes also manifest themselves in the resistivity of deformed CrMnFeCoNi alloys in the course of heating-cooling cycle. In this case, it was found that, unlike $CrMnFeCoNi_2Cu$ alloy, the resistivity of the deformed CrMnFeCoNi alloy grows after such annealing. This fact is illustrated in Fig. 5, where curve *1* describes the first heating cycle, and curve *2* the second heating cycle performed after the same specimen had been cooled down. The growth of ρ is not large in this case (about 3%), but the very fact of its growth contradicts general ideas of the influence of the annealing on the resistivity of deformed specimens; namely, ρ should decrease due to the annealing of defects that arose during the deformation process.

It was also found that the location of this section in the dependence $R(T)$ varies with the specimen heating rate. This can be seen in Fig. 6, where the dependence $R(T)/R_{700}$ is plotted in the temperature interval from 700 to 900 K. The exhibited dependences were measured at various heating rates v (from 8 to 34 K/min). One can see that the corresponding feature shifts toward lower T, as the heating rate decreases (curves *1* to *4*). This phenomenon can be considered as a process of nucleation and growth of a new phase, and the Kissinger method [15] can be applied to analyze it.

In this method, the activation energy E is determined as the slope angle tangent in the dependence $-\ln(v/T_x^2)$ versus $1/T_x$, where T_x is the temperature corresponding to the given rate v. Generally speaking, according to work [15], T_x corresponds to the maximum of the transformation rate, which is reached, when the amount of the formed phase $x \approx 0.63$. However, it can be shown that a similar method for the determination of E can also be

applied to the case where x is arbitrary, but constant [16]. A correct determination of the transformation rate on the basis of the dependences depicted in Fig. 6 is practically impossible, which is associated with rather small magnitudes of the effect. Therefore, while determining E, several T-values connected with transformations were used. These are the temperature T_s of the absolute transformation start and the temperature T_f of the absolute transformation finish (they were determined on the basis of appreciable deviations of the dependences concerned from their approximations by linear dependences before and after the transformation); the conditional temperatures of the transformation start, T_{x1}, and finish, T_{x2} (they were determined as the intersection points of different, close to linear, dependences from different transformation sections); and $T_x = (T_{x1} + T_{x2})/2$, which can conditionally be accepted as a temperature that corresponds to the maximum transformation rate.

In Fig. 7, the Kissinger plots are shown for various levels of transformation temperature determination. As one can see, all of them are close to linear. The determination error for E does not exceed 10%, which is typical of this method [16]. Along the temperature series $T_s \to T_{x1} \to T_x \to T_{x2} \to T_f$, the activation energy changes as follows: 124 ± 9 kJ/mol $\to$ $\to 197 \pm 20$ kJ/mol $\to 238 \pm 21$ kJ/mol $\to 282 \pm$ ± 23 kJ/mol $\to 246 \pm 11$ kJ/mol. The kinetics of this process will not be discussed in detail. We only note that, most likely, such features in the behavior of the activation energy can be considered, for example, as a result of various contributions to the nucleation and growth of domains.

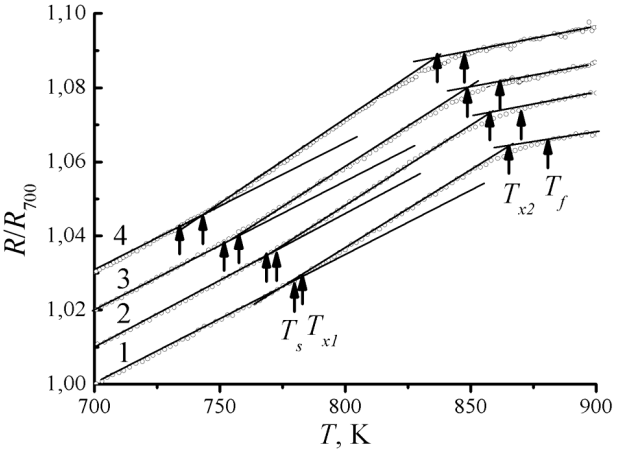

Fig. 6. Characteristic temperatures of the S-like section in the $R/R(T = 700$ K) dependences for heating rates of 34.4 (*1*), 20.4 (*2*), 13.6 (*3*), and 8.2 K/min (*4*). The plots are relatively shifted upward by $\Delta R/R_{700} = 0.01$

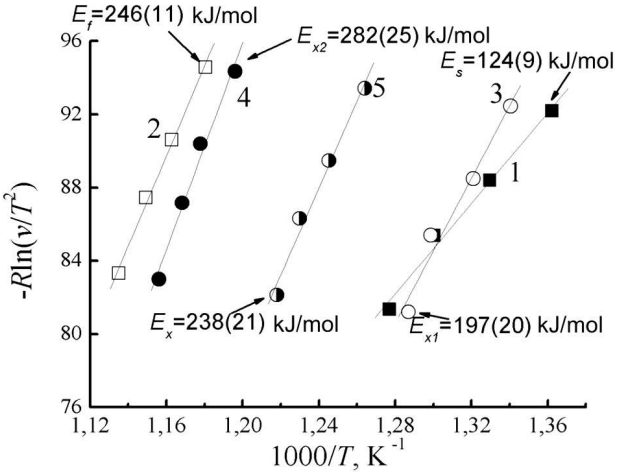

Fig. 7. Kissinger plots (dependences $\ln(v/Tx^2$ versus $1/T)$ for various determination levels of transformation temperature: T_S (*1*), T_f (*2*), T_{x1} (*3*), T_{x2} (*4*), and T_x (*5*). The values of corresponding activation energies are indicated

4. Discussion of Results

Hence, the results obtained above unambiguously indicate that HEAs, at least with the CrMnFeCoNi composition, demonstrate a non-typical dependence of the electrical resistivity at a cold deformation by rolling. The non-typical character consists in that this alloy reveals a reduction of the resistivity with the growth of a deformation, which becomes especially noticeable, when the deformation strain exceeds 80%. In this case, the TCR increases almost monotonically in the strain interval from 25 to 80%. Those features in the resistivity behavior are opposite to those observed in the case of plastic deformation for the majority of metal alloys in the crystalline state.

Really, according to the known Matthiessen rule, in the case of several scattering mechanisms, the total electrical resistivity ρ can be considered as a simple sum of electrical resistivities produced by each of the scattering mechanisms. In the most simple case, this sum is assumed to include two terms: from the scattering by phonons, $\rho_{\rm ph}$, and from the scattering by static defects, $\rho_{\rm d}$. Then

$$\rho = \rho_{\rm ph} + \rho_{\rm d}. \qquad (1)$$

The temperature dependence is contained in the term $\rho_{\rm ph}$, whereas the term $\rho_{\rm d}$ is temperature-independent, and its magnitude increases with the defect concentration. The latter depends on the plastic strain value and, consequently, should grow with ε. In this case, if there are no substantial modifications in the features of the electron structure, both $\rho_{\rm ph}$ and its temperature dependence do not change. Therefore, as ε grows, the value of ρ should increase owing to an increase of $\rho_{\rm d}$. In this case, if $d\rho_{\rm ph}/dT$ is constant, the TCR

$$\alpha = \frac{1}{\rho}\frac{d\rho}{dT} = \frac{1}{\rho}\frac{d\rho_{\rm ph}}{dT} \tag{2}$$

has to decrease owing to an increase of ρ, which is observed experimentally in the majority of cases.

Another feature of the electrical resistivity is its non-typical temperature behavior. It consists in that ρ increases, when the specimens are heated (annealed). The growth of the resistivity manifests itself at relatively low T in the form of S-like shape of the dependence $\rho(T)$. Researches show that this process is irreversible, and it originates from the processes of domain nucleation and growth. As a rule, the structure imperfection, as well as $\rho_{\rm d}$, decreases at the annealing, which explains the variation of the specific resistance in the majority of metals and alloys. But in our case, the electrical resistivity grows, although insignificantly. Furthermore, the results of researches testify that the grain recrystallization takes place in deformed CoCrFeMnNi specimens with the activation energy $E \approx 325$ kJ/mol [17, 18]. This energy is close to E_{x2}. Nevertheless, according to the results of works [17, 18], the recrystallization processes begin at temperatures higher that 600 °C (∼1000 K), which exceeds the temperature, at which the S-like feature appears in the dependences $\rho(T)$. In addition, the change of a microstructure in the deformed CoCrFeMnNi alloys becomes appreciable at $T > 800$ °C [17].

As was already mentioned, the rolling treatment gives rise to a modification in the specimen texture (see Fig. 1). However, cubic crystals have no resistance anisotropy. Therefore, expectedly, the texture itself cannot affect the electrical resistivity directly. As a result, the S-like feature in the $\rho(T)$ dependences cannot be associated with structural or phase changes, at least at the minimum spatial scale allowed by the resolution of a microstructure (see works [17, 18]) and X-ray researches carried out in this work. However, it is well known that some deformed substitutional alloys (most of them consist of transition metals) rather often reveal themselves in the so-called "K-state". Its typical manifestation just consists in the growth of the electrical resistivity at the annealing of previously cool-deformed specimens. For the first time, this phenomenon was described for a number of alloys on the basis of nickel and iron by Thomas [19], who pointed to the growth of their resistivity at a deformation and a further growth after the annealing. However, the S-like shape of the $R(T)$ curve was reported for Ni–(18–22)%Mo alloy as early as in 1938 [20]. In that case, the higher resistivity of annealed specimens was connected with the formation of stable domains characterized by a certain type of short-range order, which resulted in the appearance of additional scattering centers for conduction electrons. This unusual and complex state was later confirmed by electron microscopy and X-ray scattering researches [21, 22]. In some cases, the formation of Guinier–Preston zones [23] is considered as a prototype of this state. The calculation results also testify that not only the small size of domains with a certain type of short-range order that arise in some solid solutions at their annealing, but also the features of the *sd*-scattering in those regions are responsible for an increase of the electrical resistivity in specimens previously disordered by a deformation [24, 25].

Hence, the temperature dependence of the electrical resistivity in CrMnFeCoNi alloy completely corresponds to the behavior inherent to the K-state. The presence of a large number of transition elements can satisfy requirements to the components, for which this effect was observed. Information about the creation of domains with a definite type of short-range order could have been obtained from the researches of diffuse X-ray scattering. However, this is almost impossible for an alloy with the indicated composition because of a considerable diffusion contribution made by various components of this alloy [26]. However, the applicability of kinetic analysis to the peculiarity in the dependence $R(T)$ testifies in favor of the fact that this process runs according to the mechanism of nucleation and growth, i.e. the mechanism of formation of some new regions in the crystalline matrix.

By its order of magnitude, the activation energy of the revealed process is rather close to that of crystallization in amorphous metal alloys, and the latter pro-

cess takes place by means of just the nucleation and growth [27]. By their electrical parameters, HEAs are rather close to amorphous alloys. This fact is a result of the strong disordering in both alloy classes. However, the crystallization in amorphous alloys is usually followed by a reduction of the resistivity in the whole volume. As a result, the mechanisms of conduction electron scattering change. However, among amorphous metal alloys, there are materials, in which the crystallization process practically does not manifest itself in the dependences $R(T)$ or even brings about an increase of the electrical resistivity [28]. These are the so-called nanocrystalline amorphous alloys (of the FINMET or NANOPERM type), which testifies to the emergence of domains with a special type of short-range order in HEAs.

We may suppose that such domains do already exist in the as-fabricated alloy. During a deformation, those domains are destroyed. Moreover, the structure imperfection increases at a deformation, which is confirmed by the growth of the thermal emf. The former process should decrease the electrical resistivity, and the latter should increase it. Evidently, the competition of those two mechanisms is responsible for an insignificant reduction of the electrical resistivity, if the deformation strain is less than 80%. However, if the formation of defects saturates (the saturation of the thermal emf value), the destruction of domain regions continues, and, as a result, the electrical resistivity starts to decrease more rapidly. Concerning the temperature coefficient of the resistance, its growth is associated not only with the total reduction of the electrical resistivity [the change of $\rho_{\rm d}$ in Eq. (1)], but also with qualitative changes of scattering features (phonon spectrum, electron structure, and so on) that directly affect the temperature dependence of $\rho_{\rm ph}$ in Eq. (1).

The next temperature treatment, which is performed, when the dependence $R(T)$ is measured, leads again to the formation of such domains; therefore, the growth of the electrical resistivity is observed. According to the kinetics of this process, the formation of domains takes place by means of their nucleation and growth. Therefore, it is quite reasonable that the activation energy of this process grows: first, the nucleation process dominates, which is characterized by rather a low activation energy; then those domain regions grow, although not considerably. It is necessary to say that the diffusion processes in HEAs are rather slow, and they are characterized by rather high activation energies. For instance, for the elements of CoCrFeMnNi alloy, the diffusion activation energies Q are as follows [29]: 317.5 kJ/mol for Ni, 292.9 kJ/mol for Cr, and 288.4 kJ/mol for Mn. The activation energy E_{x2} obtained by us amounts to 282 ± 23 kJ/mol, which is slightly below Q for Ni and Cr, and practically coincides with Q for Mn. In addition, the researches of temperature features at the initial stage of plastic processes in the HEA with the same composition [30] made it possible to determine that this process is governed by the vacancy mechanism with an activation energy of 1.72 ± 0.35 eV (104 ± 21 kJ/mol), which is rather close to the energy $E_s = 124 \pm 9$ kJ/mol obtained by us.

Attention should be paid to that not only the configuration entropy plays an important role in the formation of single-phase HEAs (in the case of equiatomic alloy, it is determined as $\Delta S_{\rm mix} = = -R \ln N$, where R is the universal gas constant, and N the number of components), but also the mixing enthalpy $\Delta H_{\rm AB}^{\rm mix}$ for binary components A and B [31]. According to the data of work [32], for CoCrFeMnNi alloy, there are 10 possible values of $\Delta H_{\rm AB}^{\rm mix}$. The mixing enthalpy amounts to -7 kJ/mol for Ni and Cr and -8 kJ/mol for Ni and Mn, which are lager by absolute value that $\Delta H_{\rm AB}^{\rm mix}$ for other pairs (for instance, $\Delta H_{\rm AB}^{\rm mix} = = -5$ kJ/mol for the Co–Mn pair, being even lower for other pairs). Taking this fact into account, as well as the values obtained for activation energies, we may assume that the formation of domain structures occurs just between Ni, Cr, and Mn by means of the diffusion of Cr or Mn to Ni (however, in neither case owing to the diffusion of Cr to Mn or vice versa, because $\Delta H_{\rm AB}^{\rm mix}$ is positive for them [32]).

In work [13], the temperature dependences of the resistivity in HEAs with the composition $\mathrm{Al}_x\mathrm{CoCrFeNi}$ ($x = 0 \div 2$) and rolled to $\varepsilon = 75\%$ (at $x = 0 \div 0.875$) or $\varepsilon = 50\%$ (at $x = 0.25$) were also studied. In that case, the temperature researches were carried out in a temperature interval of 4.2–300 K. It is quite clear that the K-effect cannot manifest itself in this temperature interval. However, taking into account that the specific resistance of deformed specimens is higher in comparison with that of undeformed ones and it grows with a deformation (i.e. it can be described in the framework of the conventional ideas of the deformation effect), it is possible to believe that there is no K-effect for those alloys.

5. Conclusions

To summarize, our research of the influence of a rolling deformation has shown the following.

1. If the specimens are squeezed by rolling to a deformation strain of 90%, the phase content of CoCrFeMnNi high-entropy alloy does not change. However, the specimen texture becomes modified.

2. The behavior of the electric conductivity and the temperature coefficient of resistance for CoCrFeMnNi alloy is found to be abnormal in comparison with the corresponding dependences for the majority of traditional alloys. The anomaly consists in a reduction of the specific resistance and an increase of TCR.

3. The abnormal behavior of the resistivity can be regarded as a result of the manifestation of the K-state in this alloy. The appearance of the K-state is associated with the emergence of domains with a special type of short-range order after the annealing. Those domains can produce additional effects in the scattering of conduction electrons.

4. The formation kinetics of such domain regions shows that it can be described in the framework of the model of new phase nucleation and growth with an activation energy that varies from 124 ± 9 kJ/mol to 282 ± 23 kJ/mol. The former value is close to the activation energy at the initial stage of plastic processes in CoCrFeMnNi high-entropy alloy. This stage runs, being driven by the vacancy mechanism. The latter value is close to the diffusion activation energies of Ni, Cr, and Mn. With regard for the values of mixing enthalpies, one may assume that the formation of domains with a special type of short-range order takes place due to the diffusion of Cr or Mn to Ni.

1. J.-W. Yeh, S.-K. Chen, S.-J. Lin, J.-Y. Gan, T.-S. Chin, T.-T. Shun, C.-H. Tsau, S.-Y. Chang. Nanostructured high-entropy alloys with multiple principal elements: novel alloy design concepts and outcomes. *Adv. Eng. Mater.* **6**, 299 (2004).
2. Y. Zhang, T.T. Zuo, Z. Tang, M.C. Gao, K.A. Dahmen, P.K. Liaw, Z.P. Lu. Microstructures and properties of high-entropy alloys. *Prog. Mater. Sci.* **61**, 1 (2014).
3. O.N. Senkov, G.B. Wilks, D.B. Miracle, C.P. Chuang, P.K. Liaw. Refractory high-entropy alloys. *Intermetallics* **18**, 1758 (2010).
4. C.Y. Hsu, T.S. Sheu, J.W. Yeh, S.K. Chen. Effect of iron content on wear behaviour of $AlCoCrFe_xMo_{0.5}Ni$ high-entropy alloys. *Wear* **268**, 653 (2010).
5. Y.J. Zhou, Y. Zhang, Y.L. Wang, G.L. Chen. Solid solution alloy of $AlCoCrFeNiTi_x$ with excellent room-temperature mechanical properties. *Appl. Phys. Lett.* **90**, 181904 (2007).
6. Y.-F. Kao, T.D. Lee, S.K. Chen, Y.S. Chang. Electrochemical passive properties of $Al_xCoCrFeNi$ ($x = 0$, 0.25,0.50, 1.00) alloys in sulfuric acids. *Corros. Sci.* **52**, 1026 (2010).
7. M.-H. Tsai, J.W. Yeh, J.Y. Gan. Diffusion barrier properties of AlMoNbSiTaTiVZr high-entropy alloy layer between copper and silicon. *Thin Solid Films* **516**, 5527 (2008).
8. M.S. Lucas, L. Mauger, J.A. Munoz, Y. Xiao, A.O. Sheets, S.L. Semiatin, J. Horwath, Z. Turgut. Magnetic and vibrational properties of high-entropy alloys. *J. Appl. Phys.* **109**, 07E307 (2011).
9. K. Zhang, Z. Fu. Effects of annealing treatment on properties of $CoCrFeNiTiAl_x$multi-component alloys. *Intermetallics* **28**, 34(2012).
10. S.-K. Chen, Y.-F. Kao. Near-constant resistivity in 4.2-360 K in a B2 $Al_{2.08}CoCrFeNi$. *AIP Adv.* **2**, 012111 (2012).
11. M.-H. Tsai. Physical properties of high entropy alloys. *Entropy* **15**, 5338 (2013).
12. H.P. Chou, Y.S. Chang, S.K. Chen, J.W. Yeh. Microstructure, thermophysical and electrical properties in $Al_xCoCrFeNi$ ($0 \le x \le 2$) high-entropy alloy. *Mater. Sci. Eng.* **163**, 184 (2009).
13. Y.-F. Kao, S.-K. Chen, T.-J. Chen, P.-C. Chu, J.-W. Yeh, S.-J. Lin. Electrical, magnetic, and Hall properties of $Al_xCoCrFeNi$ high-entropy alloys. *J. Alloys Compd.* **509**, 1607 (2011).
14. M.O. Krapivka, Yu.P. Mazur, M.P. Semen'ko, S.A. Firstov. Structureof high-entropy alloys CrMnFeCoNi and $CrMnFeCoNi_2Cu$ and thermal stability of their charge transport properties. *Metallofiz. Noveish. Tekhnol.* **37**, 731 (2015) (in Ukrainian).
15. H.E. Kissinger. Reaction kinetics in differential thermal analysis. *Anal. Chem.* **29**, 1702 (1957).
16. F. Liu, F. Sommer, C. Bos, E.J. Mittemeijer. Analysis of solid state phase transformation kinetics: Models and recipes. *Int. Mat. Rev.* **52**, 193 (2007).
17. F. Otto, N.L. Hanold, E.P. George. Microstructural evolution after thermomechanical processing in an equiatomic, single-phase CoCrFeMnNi high-entropy alloy with special focus on twin boundaries. *Intermetallics* **54**, 39 (2014).
18. W.H. Liu, Y. Wu, J.Y. He, T.G. Nieh, Z.P. Lu. Grain growth and the Hall–Petch relationship in a high-entropy FeCrNiCoMn alloy. *Scripta Materialia* **68**, 526 (2013).
19. H. Thomas. Über widerstandslegierungen. *Z. Phys.* **129**, 219 (1951).
20. G. Grube, H. Schlecht. Electroconductivity and phase diagrams of binary alloys. *Z. Elektrochem.* **44**, 413 (1938).
21. E. Ruedl, P. Delavignette, S. Amelinckx. Electron diffraction and electron microscopic study of long- and short-range order in Ni_4Mo and of the substructure resulting from ordering. *Phys. Status Solidi* **28**, 305 (1968).
22. J.E. Spruiell, E.E. Stansbury. X-ray study of short-range order in nickel alloys containing 10.7 and 20.0 at.% molybdenum. *J. Phys. Chem.* **26**, 811 (1965).

23. D.M.C. Nicholson, R.H. Brown. Electrical resistivity of $Ni_{0.8}Mo_{0.2}$: Explanation of anomalous behavior in short-range ordered alloys. *Phys. Rev. Lett.* **70**, 3311 (1993).
24. Yu.N. Gornostyrev, M.I. Katsnelson. Misfit stabilized embedded nanoparticles in metallic alloys. *Phys. Chem. Chem. Phys.* **17**, 27249 (2015).
25. S. Lowitzer, D. Ködderitzsch, H. Ebert, P.R. Tulip, A. Marmodoro, J.B. Staunton. An ab initio investigation of how residual resistivity can decrease when an alloy is deformed. *Europhys. Lett.* **92**, 37009 (2010).
26. J.-W. Yeh, S.-Y. Changb, Y.-D. Honga, S.-K. Chenc, S.-J. Lin. Anomalous decrease in X-ray diffraction intensities of Cu–Ni–Al–Co–Cr–Fe–Si alloy systems with multi-principal elements. *Mater. Chem. Phys.* **103**, 41 (2007).
27. E. Nunes, J.C.C. Freitas, R.D. Pereira, A.Y. Takeuchi, C. Larica, E.C. Passamani, A.A.R. Fernandes. Phase transformation in iron/cobalt-based amorphous alloys revealed by thermal and magnetic techniques. *J. Alloys Comp.* **369**, 131 (2004).
28. Z. Stokłosa, J. Rasek, P. Kwapuliński, G. Haneczok, G. Badura, J. Lelatko. Nanocrystallization of amorphous alloys based on iron. *Mater. Sci. Eng. C* **23**, 49 (2003).
29. K.Y. Tsai, M.H. Tsai, J.W. Yeh. Sluggish diffusion in Co–Cr–Fe–Mn–Ni high-entropy alloys. *Acta Mater.* **61**, 4887 (2013).
30. C. Zhu, Z.P. Lu, T.G. Nieh. Incipient plasticity and dislocation nucleation of FeCoCrNiMn high-entropy alloy. *Acta Mater.* **61**, 2993 (2013).
31. F. Otto, Y. Yang, H. Bei, E.P. George. Relative effects of enthalpy and entropy on the phase stability of equiatomic high-entropy alloys. *Acta Mater.* **61**, 2628 (2013).
32. A. Takeuchi, A. Inoue. Classification of bulk metallic glasses by atomic size difference, heat of mixing and period of constituent elements and its application to characterization of the main alloying element. *Mater. Trans.* **46**, 2817 (2005).

Received 29.02.16.
Translated from Ukrainian by O.I. Voitenko

Ю.П. Мазур, Р.В. Остапенко, М.П. Семенько

ВПЛИВ ХОЛОДНОЇ
ПЛАСТИЧНОЇ ДЕФОРМАЦІЇ НА ЕЛЕКТРООПІР
ВИСОКОЕНТРОПІЙНОГО СПЛАВУ CrMnFeCoNi

Р е з ю м е

Досліджено вплив холодної деформації вальцюванням на електротранспортні властивості високоентропійного сплаву (ВЕСу) CrMnFeCoNi. Показано, що з ростом величини деформації при вальцюванні, ε, питомий електроопір, ρ, цього сплаву зменшується, а температурний коефіцієнт опору, α, зростає. При цьому, методом рентгенівської дифракції ніяких фазових змін не виявлено. Така поведінка ρ та α від ε відрізняється від поведінки цих величин більшості традиційних металевих сплавів. Встановлено, що температурна залежність електроопору при нагріванні деформованих зразків характеризується аномальною S-подібною формою. По положенню таких S-аномалій при різних швидкостях нагрівання, методом Кіссінджера визначено енергію активації E_a процесу, що відповідає за аномалію. Форма залежності $\rho(T)$ та величина E_a дають підставу віднести такі особливості поведінки ρ деформованих зразків до існування в дослідженому ВЕСі "К-стану", що проявляється в деяких деформованих сплавах на основі перехідних металів. Обговорено можливі термодинамічні причини виникнення цього стану.